Journal of Physics: Conference Series **131** (2008) 012012 doi:10.1088/1742-6596/131/1/012012

Orbits and origins of the young stars in the central parsec of the Galaxy

J R Lu[1], A M Ghez[1,2], M Morris[1], S D Hornstein[1,3] and K Matthews[4]

[1] UCLA Department of Physics and Astronomy, Los Angeles, CA 90095-1562

[2] UCLA Institute of Geophysics and Planetary Physics, Los Angeles, CA 90095-1565

[3] CASA, Department of Astrophysical and Planetary Sciences, University of Colorado, Boulder, CO 80309

[4] COO, California Institute of Technology, MS 320-47, Pasadena, CA 91125

E-mail: `jlu, ghez, morris, seth@astro.ucla.edu, kym@astro.caltech.edu`

Abstract. We present new proper motions from the 10 m Keck telescopes for a puzzling population of massive, young stars located within a parsec of the supermassive black hole at the Galactic Center. Our proper motion measurements have uncertainties of only 0.07 mas yr^{-1} (3 km s^{-1}), which is $\gtrsim$ 7 times better than previous proper motion measurements for these stars, and enables us to measure accelerations as low as 0.2 mas yr^{-2} (7 km s^{-1} yr^{-1}). These measurements, along with stellar line-of-sight velocities from the literature, constrain the true orbit of each individual star and allow us to directly test the hypothesis that the massive stars reside in two stellar disks as has been previously proposed. Analysis of the stellar orbits reveals only one disk of young stars using a method that is capable of detecting disks containing at least 7 stars. The detected disk contains 50% (38 of 73) of the young stars, is inclined by $\sim 115°$ from the plane of the sky, and is oriented at a position angle of $\sim 100°$ East of North. The on-disk and off-disk populations have similar K-band luminosity functions and radial distributions that decrease at larger radii as $\propto r^{-2}$. The disk has an out-of-the-disk velocity dispersion of 28 $\pm$ 6 km s^{-1}, which corresponds to a half-opening angle of $7° \pm 2°$, and several candidate disk members have eccentricities greater than 0.2. Our findings suggest that the young stars may have formed *in situ* but in a more complex geometry than a simple thin circular disk.

1. Introduction

The center of our Galaxy harbors not only a supermassive black hole of mass, $M_{SgrA*} \sim 4 \times 10^6$ M$_\odot$ ([1], A. M. Ghez, submitted), but also a population of massive (10-120 M$_\odot$), young ($\lesssim$10-100 Myr) stars whose existence is a puzzle (e.g. [2, 3]). The origin of such young stars has been difficult to explain since the gas densities observed today in the Galactic Center are orders of magnitude too low for a gas clump to overcome the extreme tidal forces and collapse to form stars [4, 5]. Proposed resolutions to this "paradox of youth" include scenarios in which these young stars formed in a massive, self-gravitating accretion disk that was once present around the black hole [6] or alternatively, formed far from their current positions, outside the black hole's sphere of influence, as part of a massive star cluster which spiraled in via dynamical friction and deposited the most massive stars where we see them today [7].

Insight into the origins of the massive, young stars may be obtained through observations of the spatial distribution and stellar dynamics of this population. Already, high-resolution infrared imaging and spectroscopy have shown that a significant part of the young stars between

$0''.5$ and $14''$(0.02-0.6 pc) projected distance from Sgr A* exhibit coherent rotation [8]. Analyses of the statistical properties of the three-dimensional velocity vectors for these stars suggest that they lie in a clockwise-rotating disk [6] and perhaps also a counter-clockwise-rotating disk [9] that is nearly perpendicular to the first, with the disks extending from $\sim 0''.8$ to at least $7''$[3]. Both *in situ* gas disk and in-spiraling star cluster formation scenarios have been used to explain the kinematics of this young star population and to predict that the stars should lie in a common orbital plane. However, the presence of two stellar disks with similarly aged populations requires either two nearly concurrent gas disks or two infalling star clusters; and both of these scenarios are difficult to produce. Therefore, to understand the recent star formation history, it is critical to measure the orbital planes of individual stars in order to confirm the existence of the two stellar disks previously derived from a statistical analysis of velocity vectors alone. Furthermore, *in situ* gas disk and inspiraling star cluster formation scenarios predict different structures and evolutions for the resulting stellar disk, particularly with respect to the eccentricities and radial distribution of stars within the disk. Current models of a self-gravitating gas disk around the supermassive black hole at the center of the Galaxy typically produce disks with a steep radial profile (disk surface density,$\Sigma \propto r^{-2}$; [10]) on circular orbits since the gas disk is rapidly circularized [11, 12, 13]. On the other hand, an inspiraling star cluster would dissolve into a disk of stars with a flatter radial profile ($\Sigma \propto r^{-0.75}$; [14]) whose orbital eccentricities would reflect the eccentricity of the cluster's orbit, which could be either circular or eccentric [15, 16, 17, 18, 19, 14]. Previous measurements of the radial distribution of young stars yield a steep radial profile consistent with *in situ* formation [3]. Also, the eccentricities of the stars have previously been estimated from observations by assuming that the stars orbit in a disk; however, there are conflicting results claiming that the stars in the clockwise-rotating disk are on nearly circular orbits [3] or on eccentric orbits [20]. Determining the radial profile and stellar eccentricities of stars in a disk may provide observational constraints on the origin of the young stars.

We present an improved proper motion study that yields an order of magnitude more precise proper motions and the first measurement of accelerations in the plane of the sky for stars outside the central arcsecond. By combining the stellar positions, proper motions, radial velocities, and accelerations, we estimate stellar orbital parameters and test whether the young stars reside on one or two stellar disks in a more direct manner than previous methods using only velocity information. This provides a *direct* test of the existence, membership, and properties of these disks. The observations and astrometric analysis are briefly described in §2. Orbit results are presented in §3 and a discussion of the implications for the origin of the massive, young stars at the Galactic Center is presented in §4. Further details for these results are also presented in J. R. Lu et al. (submitted).

2. Observations and Analysis

This study utilizes 29 epochs of high-resolution, infrared images of the Galaxy's central stellar cluster, which were taken from 1995 to 2005 using both speckle and laser guide star adaptive optics (LGS AO) observing techniques on the W. M. Keck 10 m telescopes. Prior to LGS AO observations, the NIRC speckle data sets contained a small amount of residual geometric distortion. Although this distortion is small near the center of the images, where Sgr A* and the central arcsecond sources are located; the astrometric accuracy of stars at larger radii is dominated by this residual distortion term. Our LGS AO observations offer a substantial improvement in data quality over speckle imaging and, of particular interest to this study, have well characterized distortion. Simultaneous speckle and LGS AO observations have enabled us, for the first time, to fully characterize and correct optical distortion in the speckle data (Figure 1) resulting in an astrometric accuracy that is consistent over the entire field of view.

The goal of this analysis is to obtain high precision astrometry for a sample of young stars

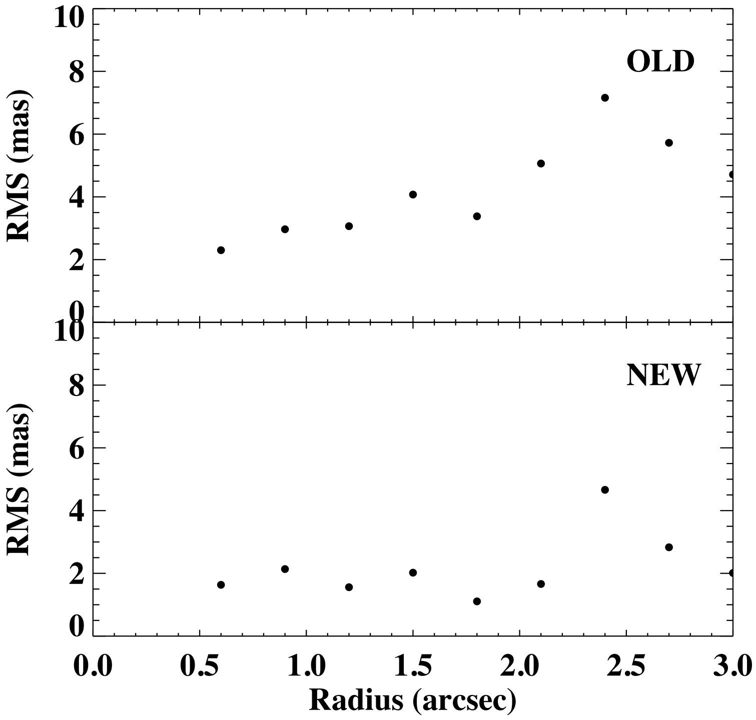

Figure 1. The improvement in positional accuracy at large radii as a result of correcting geometric distortion in speckle data sets. To characterize the systematic positional uncertainty, we take each star at each epoch and calculate the residual positional offset, which is defined as the difference between the measured position and the position as determined by the best fit velocity ($x = x_o + v * \Delta t$). Then the RMS of the residuals is calculated across all epochs for each star. All stars' resulting RMS values are sorted by the distance between the star and Sgr A* (which was at the center of the images) and then averaged over radius bins of $0''.3$. The radial trend is shown for data prior to the new distortion correction (top) and after the new distortion correction (bottom).

that are candidate disk members and have existing radial velocity measurements [3]. We define a *primary sample* of 32 young stars found in our astrometric data sets that have projected radii between $0''.8$ and $3''.5$. We also define an *extended sample* that includes the remaining 41 young stars found by [3] at larger radii that fall outside our field of view. For the primary sample we measure the positions, velocities, and accelerations in the plane-of-the-sky from our astrometric data. The acceleration measurements for all but one star, S0-15, are statistically consistent with zero; however, the acceleration limits provide important constraints on the allowed orbits for each star. For the extended sample we adopt position and proper motion data from the literature [3] that has an order of magnitude lower precision and lacks any constraints on accelerations.

We determined individual stellar orbits for the sample of young stars by assuming a Keplerian orbit model in which the gravitational potential arises from a single dominant point mass situated at the dynamical center of our Galaxy. For this analysis, we assume that the central point mass is a black hole with characteristics determined by analysis of the orbit of the star S0-2, which has been observed for nearly one complete revolution (A. M. Ghez et al. 2008, submitted). Our

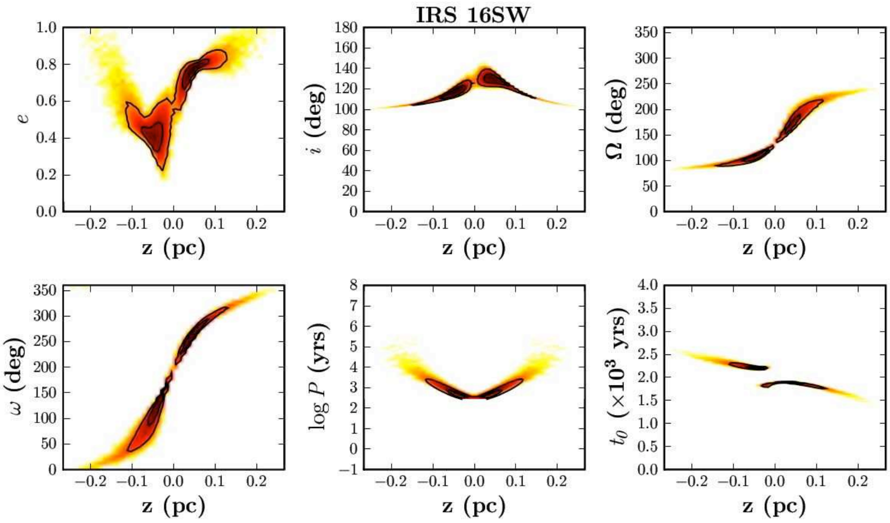

Figure 2. The range of allowed orbital parameters for IRS 16SW as determined from the observed two-dimensional position in the plane of the sky, the three-dimensional velocity, and the acceleration in the plane of the sky. The probability distribution for each orbital parameter is plotted against the unknown line-of-sight distance, z, and is determined by sampling from a gaussian distribution for each of the observed quantities and analytically converting to the standard orbital elements. High density (dark) regions represent the most probable values for each orbital parameter and the resulting 1σ and 2σ contours are shown as black lines.

proper motion analysis yields information on five kinematic variables, including two positions, two velocities, and one acceleration. The sixth kinematic variable comes from radial velocities measured by [3]. The plane-of-the-sky acceleration can be converted into a line-of-sight distance that, when combined with the projected distance, gives the full three-dimensional position for a star. For stars in the extended sample, accelerations are not measured, and instead a uniform range of all possible accelerations for bound orbits are considered. Therefore, the six measured quantities and the known properties of the black hole can be translated directly into 6 standard orbital elements (i, e, ω,Ω, P, t_o) using a Monte Carlo simulation that produces the most probable orbital parameters and their uncertainties (see Figure 2 for an example).

3. Results

3.1. Detection of the Clockwise Disk

A large number of stars appear to share a common orbital plane based on our analysis, which has no prior assumption about the existence of a disk. The orientation of a star's orbital plane can be described by a unit vector originating at Sgr A*'s position and pointing normal to the orbital plane ($\vec{n}$); and, this normal vector's direction can be expressed by the inclination angle (i) and the angle to the ascending node (Ω). From the Monte Carlo simulations, the joint two-dimensional probability density function, PDF(i,Ω), is constructed by binning the resulting i and Ω values in a two-dimensional histogram with equal solid angle bins using the HEALpix framework [21]. Figure 3 shows, for all stars, the contours for the 68% confidence region of PDF(i,Ω), which, on average, covers a solid angle of $SA_{\vec{n}}$ ∼0.2 steradian (sr) in the primary sample and 0.6 sr in the extended sample, which has larger proper motion uncertainties. Stars with acceleration limits that are smaller than that allowed for bound orbits have two isolated solutions because small line-of-sight distances (z) are not permitted and at large line-of-sight

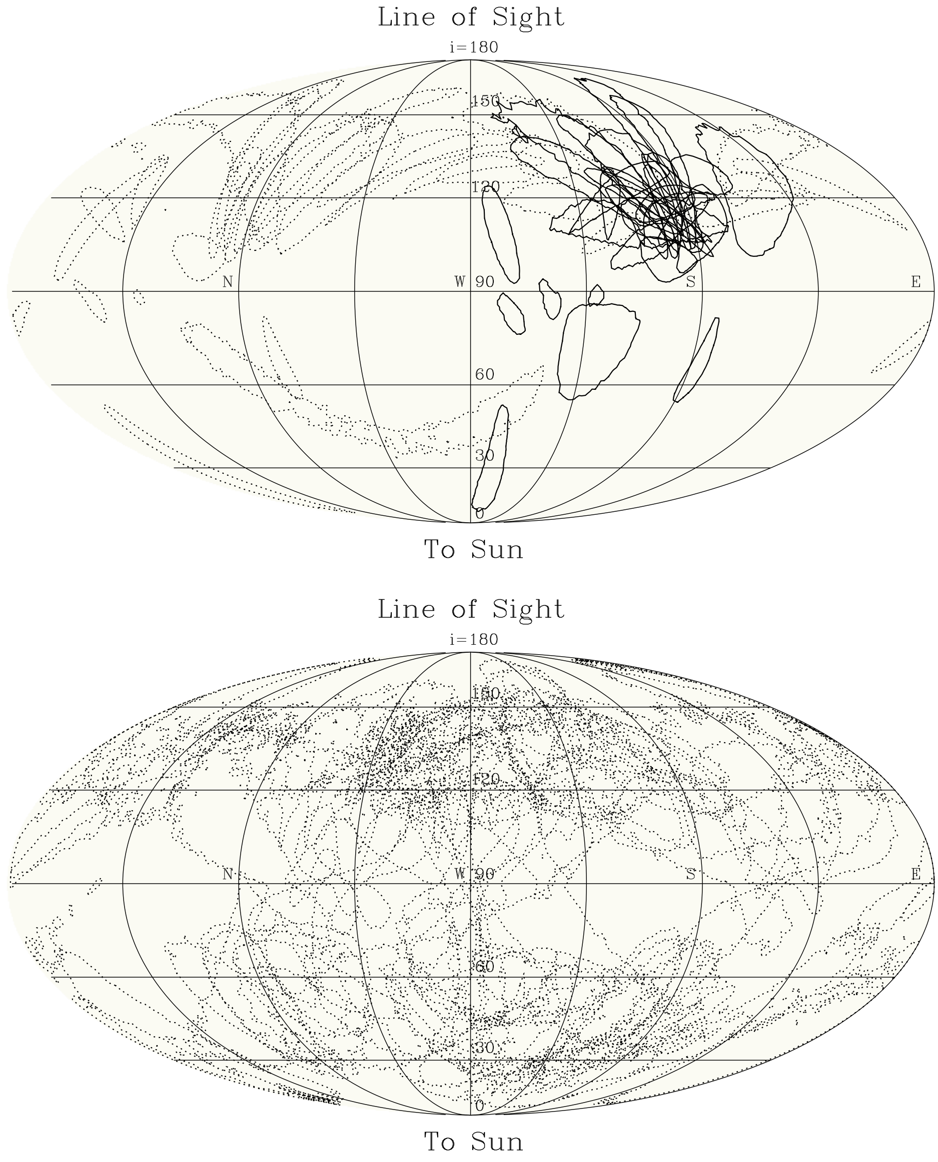

Figure 3. The 1σ contours of all stars' probability distribution functions for the orientation of their orbital planes. This shows the distribution of stellar orbit orientations around the sky. The primary sample is plotted on the *top* and if there are degenerate solutions for a given star, then one solution is plotted with a solid line and the other with a dashed line. Additional sources found only in the extended sample are plotted on the *bottom* and are plotted with dashed lines as there are no acceleration constraints and each star has a single solution with large uncertainties.

distances the $+z$ and $-z$ solutions asymptote to two different values of Ω (see Figure 2). Despite this degeneracy, the clockwise (i=90°-180°) stars' normal vectors appear to cluster around a common point indicating that many of these stars lie on a common orbital plane.

To quantify the clustering of orbital planes, we calculate the density of normal vectors in the sky as viewed from Sgr A*. A peak in the density of normal vectors is detected at $i = 115° \pm 3°$

and $\Omega = 100° \pm 3°$, which provides direct evidence of a common orbital plane without any prior assumptions (see Figure 4). We also note that including or not including the stars from the extended sample in this analysis does not change the position of the peak. The mean density of normal vectors at the peak is 0.016 stars deg^{-2} with a negligible uncertainty on the mean value ($< 10^{-4}$ stars deg^{-2}). The significance of the peak is determined by comparing the background density of normal vectors, which is defined by the average (0.001 stars deg^{-2}) and standard deviation (0.0008 stars deg^{-2}) of all other pixels on the sky after first rejecting those pixels ($\sim$0.25 sr) that are high outliers (more than three standard deviations). For the primary sample, the density peak is $\sim 19\sigma$ above the observed background density and $\gtrsim$20 times higher than the density expected if the 32 stars were isotropically distributed over 4π steradians. Including the extended sample lowers the significance to $\sim 8\sigma$ since there are no acceleration constraints for these stars. Thus we conclude that there is a statistically significant common orbital plane of young stars.

The analysis of both the primary and extended samples shows that $\sim$50% of the young stars reside on the CW disk and there is no statistically significant change ($> 3\sigma$) in the fractional number of disk stars at different radii. For reference, the 73 young stars in the combined sample are distributed on the plane of the sky with a surface density that decreases with radius as $\rho^{-2.1\pm0.4}$. Within a projected radius of 3", the fraction of disk members is 72% $\pm$ 9% (18 out of 25) and at projected radii larger than 3", the fraction of disk members is 42% $\pm$ 7% (20 out of 48). Given the small number of known young stars, Poisson statistics indicate that this change in the fraction of disk members is only marginally statistically significant at the 2.6σ level. Likewise, the projected surface density for the on-disk and off-disk populations shown no significant difference from each other or from that of the total population. Thus the number of disk members does not change dramatically with radius and roughly half of the young stars reside on the CW disk.

The K-band luminosity function (KLF) of the young stars also does not change significantly with radius or change for stars on and off the disk. To compare the KLF as a function of radius, the entire extended sample of young stars is divided into a near sample (r $< 3\farcs5$) and a far sample (r $\geq 3\farcs5$) and the KLF is constructed for each. A two-sample KS test yields a probability of 46% that the near and far samples have the same KLF. Similarly, the KLF is constructed for stars on and off the disk and a two-sample KS test yields a probability of 74% that the on-disk and off-disk samples have the same KLF. Finding more young stars will allow for a more detailed comparison of the KLF for different subsets within the young stars population.

3.2. Limits on Additional Stellar Disks

Analysis of both the primary and extended sample reveals no significant over-density at the proposed orientation of the counter-clockwise disk. Of the 73 stars in the combined sample, at least 34 are not on the clockwise disk and thus we compare the density observed in the region of the proposed counter-clockwise disk to that expected for an isotropic distribution of 34 stars. The observed density of normal vectors in the region of the counter-clockwise disk is 2.4×10^{-3} stars deg^{-2}, which is only a factor of 3 above what is expected for an isotropic distribution and is less than 1σ above the background over the rest of the sky (excluding the clockwise peak). This density of normal vectors corresponds to only 3 stars within 19° of the supposed disk, where 19° is the disk thickness proposed by [3], and is consistent with random fluctuations of an isotropic distribution given the current uncertainties on $\vec{n}$. We estimate that this analysis is capable of revealing, at the 3σ level, a stellar disk with more than 7 stars within a solid angle cone of radius = 19° at the location of the proposed CCW disk; thus the proposed CCW disk containing 17 stars as suggested by [3] should have been detected with this approach. The distribution of young stars resulting from our study supports the hypothesis of a single, clockwise disk plus a more isotropically distributed population.

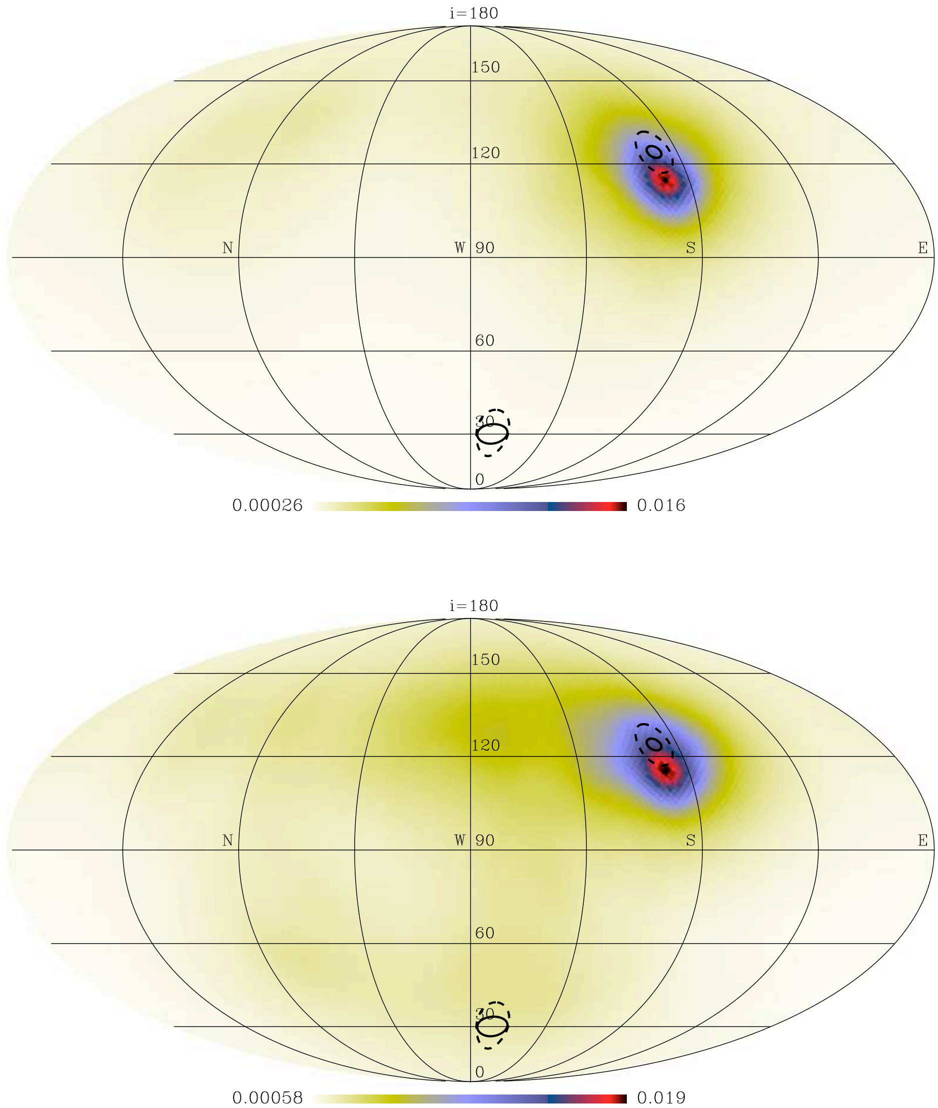

Figure 4. The density of normal vectors to the orbital planes of the stars in our primary (*top*) and extended (*bottom*) samples. Densities are indicated in colors (stars deg^{-2}) on a linear scale and the peak indicates an over-density of stars with similar orbital planes. Over-plotted in black are the candidate orbital planes as proposed by [6] and [9] with updated values from [3] for the candidate plane normal vector and uncertainties (solid black) and the disk thickness (dashed black) shown as solid angles of 0.05 sr and 0.09 sr for the clockwise and counter-clockwise disks respectively.

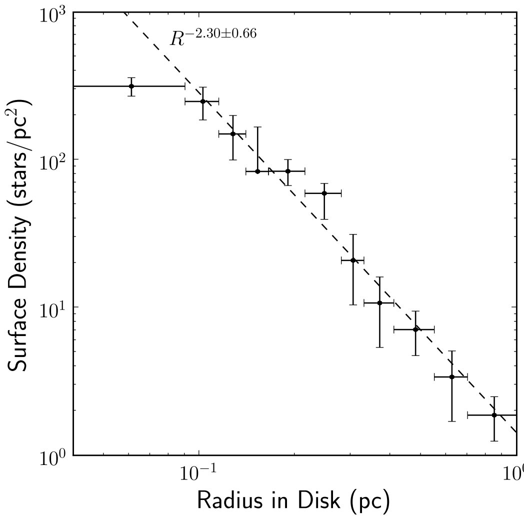

Figure 5. The radial distribution of stars within the disk plane for the extended sample. The best fit line is shown (*dashed*) and was constructed by excluding the first data point and the last three data points where field of view limitations may affect the distribution.

3.3. Properties of the Clockwise Disk

We now examine, in detail, the properties of the detected clockwise disk. With the identification of a single stellar disk and a candidate list of disk members, we investigate the following: (1) the thickness of the disk, (2) the radial profile of the disk, and (3) the eccentricities of stars in the disk. These properties are critical for distinguishing between *in situ* and infalling cluster formation scenarios, as well as for understanding the dynamical evolution of the young stars both on and off the disk. The observed disk of young stars has a significant intrinsic thickness; however, the vertical velocity dispersion is less than previously determined. The intrinsic out-of-the-plane velocity dispersion is 28 $\pm$ 6 km s^{-1}, which can be expressed as a vertical scale height of $h/r = 0.08 \pm 0.02$ or a half-opening angle of $7° \pm 2°$. We find that the surface density of stars in the disk falls off rapidly as a function of radius. The azimuthally averaged surface density on the disk is shown for the extended sample in Figure 5 and has a best-fit power-law profile of $r^{-2.3\pm0.7}$. This is consistent with the previous results [3], but accounting for the finite disk thickness, our analysis yields a larger uncertainty on the power-law index. A few candidate disk stars show evidence for eccentric orbits. When considering all possible orbital solutions, the resulting eccentricity ranges show that 2 candidate disk members from the primary sample have 99.7% confidence eccentricity lower limits of greater than 0.2. Restricting the possible orbital solutions to only those having normal vectors oriented within 10° of the disk normal vector increases the number to 8 candidate disk members within the primary sample with 99.7% confidence eccentricity lower limits larger than 0.2. Thus we find high-eccentricity stars in the disk, similar to the analysis of [20] in which they assumed an infinitely thin disk. However, our analysis incorporates the finite thickness of the disk and places statistical errors on the eccentricities for individual stars. The average eccentricity of the entire population is not yet well constrained. While the characteristic disk eccentricity peaks at e=0.22, it is consistent with e=0.0 $-$ 0.8 at the 1σ level, reflecting the large eccentricity uncertainties for the majority of the candidate disk members.

4. Discussion

The kinematic analysis of the young stars in the central parsec around our Galaxy's supermassive black hole has implications for the recent star formation history in this region. Our first attempt at determining individual orbits for young stars that reside outside the central arcsecond shows definitive evidence for the clockwise-rotating disk that was suggested by [6] and was subsequently refined by [9] and [3]. Our results do not show a statistically significant second disk. The presence of a single stellar disk eliminates the need to invoke two distinct starburst events occurring roughly 6 Myr ago and greatly simplifies the demands on both *in situ* and infalling cluster scenarios. For instance, in the self-gravitating gas disk scenario, the detection of only a single stellar disk lifts the requirement for a second disk to rapidly build up gas, fragment, and form stars within 1-2 Myr of the formation of the first disk. Likewise, for the infalling cluster scenario, the presence of only one stellar disk means that the frequency of such infall events is half that required for the existence of two disks. Our confirmation of only one stellar disk suggests that all of the young stars within the central parsec may have formed in a single burst of star formation. Any formation scenario must also explain the observed thickness of the clockwise disk and the presence of high eccentricity stars both in and out of the disk plane. There are open questions as to how $\sim$50% of all young stars can be perturbed out of the disk plane and whether the apparent compact cluster, IRS 13, which is not part of the stellar disk, requires a separate star formation or dynamical event. Future directions include (1) obtaining new LGS AO data sets with improved astrometry to measure accelerations for the young stars at all radii and (2) identifying new young stars within the central parsec in order to better constrain the orbital properties of these stars and to study in detail the distribution of eccentricities and semi-major axes for stars both in and out of the disk.

Acknowledgments

Support for this work was provided by J.R.L.'s NSF Graduate Research Fellowship, NSF grant AST-0406816, and the NSF Science & Technology Center for AO, managed by UCSC (AST-9876783). The W.M. Keck Observatory is operated as a scientific partnership among the California Institute of Technology, the University of California and the National Aeronautics and Space Administration. The Observatory was made possible by the generous financial support of the W.M. Keck Foundation.

References

[1] Eisenhauer F, Genzel R, Alexander T, Abuter R, Paumard T, Ott T, Gilbert A, Gillessen S, Horrobin M, Trippe S, Bonnet H, Dumas C, Hubin N, Kaufer A, Kissler-Patig M, Monnet G, Ströbele S, Szeifert T, Eckart A, Schödel R and Zucker S 2005 *ApJ* **628** 246–259 (*Preprint* astro-ph/0502129)
[2] Allen D A, Hyland A R and Hillier D J 1990 *MNRAS* **244** 706–713
[3] Paumard T, Genzel R, Martins F, Nayakshin S, Beloborodov A M, Levin Y, Trippe S, Eisenhauer F, Ott T, Gillessen S, Abuter R, Cuadra J, Alexander T and Sternberg A 2006 *ApJ* **643** 1011–1035 (*Preprint* astro-ph/0601268)
[4] Sanders R H 1992 *Nature* **359** 131–+
[5] Morris M 1993 *ApJ* **408** 496–506
[6] Levin Y and Beloborodov A M 2003 *ApJL* **590** L33–L36
[7] Gerhard O 2001 *ApJL* **546** L39–L42
[8] Genzel R, Pichon C, Eckart A, Gerhard O E and Ott T 2000 *MNRAS* **317** 348–374
[9] Genzel R, Schödel R, Ott T, Eisenhauer F, Hofmann R, Lehnert M, Eckart A, Alexander T, Sternberg A, Lenzen R, Clénet Y, Lacombe F, Rouan D, Renzini A and Tacconi-Garman L E 2003 *ApJ* **594** 812–832
[10] Lin D N C and Pringle J E 1987 *MNRAS* **225** 607–613
[11] Milosavljević M and Loeb A 2004 *ApJL* **604** L45–L48 (*Preprint* astro-ph/0401221)
[12] Nayakshin S and Cuadra J 2005 *AAP* **437** 437–445 (*Preprint* astro-ph/0409541)
[13] Levin Y 2007 *MNRAS* **374** 515–524
[14] Berukoff S J and Hansen B M S 2006 *ApJ* **650** 901–915
[15] Portegies Zwart S F, McMillan S L W and Gerhard O 2003 *ApJ* **593** 352–357

[16] McMillan S L W and Portegies Zwart S F 2003 *ApJ* **596** 314–322 (*Preprint* astro-ph/0304022)
[17] Kim S S and Morris M 2003 *ApJ* **597** 312–322
[18] Kim S S, Figer D F and Morris M 2004 *ApJL* **607** L123–L126
[19] Gürkan M A and Rasio F A 2005 *ApJ* **628** 236–245 (*Preprint* astro-ph/0412452)
[20] Beloborodov A M, Levin Y, Eisenhauer F, Genzel R, Paumard T, Gillessen S and Ott T 2006 *ApJ* **648** 405–410 (*Preprint* arXiv:astro-ph/0601273)
[21] Górski K M, Hivon E, Banday A J, Wandelt B D, Hansen F K, Reinecke M and Bartelmann M 2005 *ApJ* **622** 759–771 (*Preprint* astro-ph/0409513)